The Plant Journal (2000) **22**(1), 9–17

Ion currents involved in early Nod factor response in *Medicago sativa* root hairs: a discontinuous single-electrode voltage-clamp study

Armen Kurkdjian[1,*,†], François Bouteau[2,†], Anne-Marie Pennarun[2], Monique Convert[2], Daniel Cornel[2], Jean-Pierre Rona[2] and Ulrike Bousquet[2]

[1]*Institut des Sciences Végétales, Centre National de la Recherche Scientifique, Bât 22, Avenue de la Terrasse, 91198 Gif-sur-Yvette Cedex, France, and*

[2]*Université Paris 7, Electrophysiologie des Membranes LPCMSP, CASE 7069, Tour 54–64, 2 place Jussieu, 75251 Paris Cedex 05, France*

Received 22 November 1999; revised 4 February 2000; accepted 8 February 2000.
*For correspondence (fax +33 1 69 82 37 68; e-mail armen@isv.cnrs-gif.fr).
†Both authors contributed equally to the work.

Summary

Nod factor [NodRm-IV(Ac,S)], isolated from the bacterium *Rhizobium meliloti*, induces a well-known depolarization in *Medicago sativa* (cv Sitel) root hairs. Analysis of this membrane response using the discontinuous single-electrode voltage-clamp technique (dSEVC) shows that anion channel, K^+ channel and H^+-ATPase pump currents are involved in young growing root hairs. The early Nod-factor-induced depolarization is due to increase of the inward ion current and inhibition of the H^+ pump. It involved an instantaneous inward anion current (IIAC) and/or a time-dependent inward K^+ current (IRKC). These two ion currents are then down-regulated while the H^+ pump is stimulated, allowing long-term rectification of the membrane potential (E_m). Our results support the idea that the regulation of inward current plays a primary role in the Nod-factor-induced electrical response, the nature of the ions carried by these currents depending on the activated anion and/or K^+ channels at the plasma membrane.

Introduction

The interaction between the soil bacteria *Rhizobium* and legume root hairs results in the development of nitrogen-fixing nodules (for review, see Mylona *et al.*, 1995). In response to flavonoids excreted by roots, bacterial genes are involved in the synthesis of lipo-oligosaccharide signal molecules, termed Nod factors (Long, 1996 and refs therein). These molecules, isolated from bacterial supernatant cultures (Lerouge *et al.*, 1990; Schultze *et al.*, 1992; Truchet *et al.*, 1991), are perceived at very low concentrations by root cells, suggesting a receptor-mediated mechanism (Niebel *et al.*, 1997). They induce (i) an early plasma membrane depolarization (Ehrhardt *et al.*, 1992; Felle *et al.*, 1995; Kurkdjian, 1995), (ii) modification of the arrangement of actin microfilaments (Cardenas *et al.*, 1998; de Ruijter *et al.*, 1999) leading to root hair deformation (Lerouge *et al.*, 1990; Spaink *et al.*, 1991; Truchet *et al.*, 1991), and (iii) gene expression (Bauer *et al.*, 1997; Geurts and Franssen, 1996; Horvath *et al.*, 1993; Journet *et al.*, 1994), that prepares for (iv) the entry of bacteria into the root via infection threads (Relic *et al.*, 1994).

Changes in membrane potential (E_m) represent an early response of plant cells to various signals (hormones, elicitors, light and other environmental signals) mediated by ion fluxes (mainly H^+, Cl^-, Ca^{2+} and K^+), which are activated or inhibited (for review, see Ward and Schroeder, 1997). Concerning Nod factor, the early membrane depolarization could be due to a positive electrical net current entering the root hair or/and to a negative one leaving it. The long-term rectification of E_m could be due either to regulation of the currents previously activated, or to activation of new channel or pump currents.

Data from a study by Pingret *et al.* (1998) provide evidence favouring a role for G proteins in Nod factor signal transduction. The putative pathway described also involved phospholipase C activation, allowing calcium influx/release in the cytosol. The early involvement of calcium influx in Nod factor signalling was also shown by

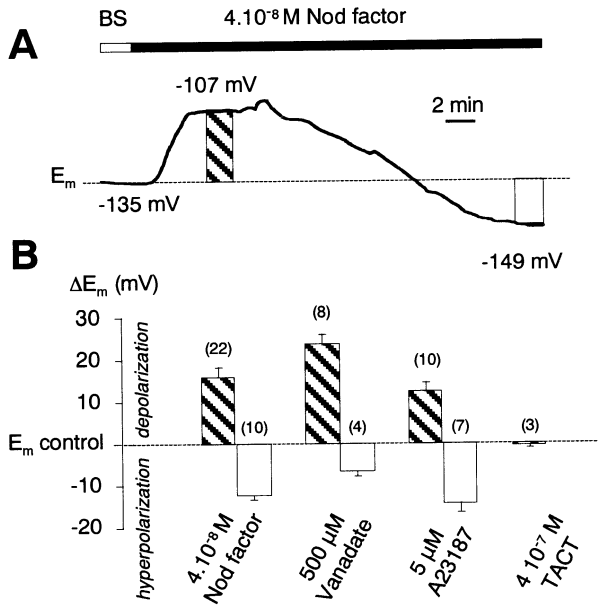

Figure 1. Nod factor [NodRm-IV(Ac,S)]-induced changes in the electrical membrane potential in a *Medicago* root hair.
Comparison with vanadate, A23187 and TACT.
(A) Recording of the membrane potential (E_m). A whole plantlet (29 h old) was perfused with standard buffer solution (BS) (pH 6.0) (except for vanadate where the pH was lowered to 5.5). The bar illustrates the time when Nod factor (4×10^{-8} M) was added to the bath solution.
(B) ΔE_m (mV) corresponding to the maximal amplitudes of depolarization and hyperpolarization after treatment with Nod factor (as indicated in (A)), vanadate (500 μM), A23187 (5 μM) or TACT (4×10^{-7} M). The numbers in parentheses correspond to the number of experiments for each treatment.

the use of calcium- sensitive dyes (Cardenas *et al.*, 1999; Ehrhardt *et al.*, 1996; Gehring *et al.*, 1997) and by external ion-selective microelectrode studies (Felle *et al.*, 1998; Felle *et al.*, 1999). According to these authors, the calcium influx is followed after a few seconds by an increase of chloride efflux and a decrease of H^+ efflux, and then a delayed increase of K^+ efflux, accounting for the electrical membrane response induced by the Nod factor. However, the nature of the ion channel currents underlying the dynamic functioning of the ion exchange systems has not yet been adequately studied. To address this question, we used a discontinuous single-electrode voltage-clamp technique for an *in situ* investigation (Bouteau *et al.*, 1999). In this paper, we provide evidence that anion and potassium channel currents together with H^+ pump currents are at the origin of the electrical response induced by Nod factor.

Results

Characteristics of the currents

A previous electrophysiological and pharmacological study (Bouteau *et al.*, 1999) identified several ion channel currents in the plasma membrane of *Medicago* root hairs *in situ*: a K^+ inward-rectifying time-dependent current (IRKC) (also functioning as a K^+ efflux pathway which disappears towards positive potential values); an outward-rectifying time-dependent K^+ current (ORKC) allowing K^+ efflux under strong depolarizations and an instantaneous inward anion current (IIAC). In spite of the care taken to choose uniform root hairs in terms of size and morphology, several different electrical signatures were routinely recorded. This variability could frequently be observed for two neighbour hairs on the same root. Thus, this variability could not be due to the development of the hair or to the season. Furthermore, the different signatures were recorded whatever the impalement position, in the apex of the growing tip or in the base of the root hair. The ORKC was present in less than 4% of recordings. Only 6% of the cells displayed only the IRKC. The other recordings showed an instantaneous inward anion current (IIAC) associated with the IRKC. The amplitude of IIAC ranged from 57 to 100% of the total current. A pharmacological study using inhibitors, which are rarely specific for only one transport system, appeared to be of limited use to discriminate these currents which constitute variable amounts of the total current. Thus, we initially classified the nature of the current displayed by each root hair using as major criteria the current kinetics and the threshold for voltage activation (near to E_K or E_{A-}, respectively, equilibrium potential for K^+ and anions, see Bouteau *et al.*, 1999). To assess the role of IIAC and IRKC, we choose to work on root hairs showing predominantly one of these currents to investigate the action of Nod factor on these ion channel currents. However, the amplitude of currents we recorded was highly variable from one root hair to another. Under these conditions, it was sometimes difficult to be sure that no low-amplitude IRKC current was present with a large IIAC component which imposed the threshold voltage. However, additional data are provided for Nod factor effect on root hairs displaying a total current with both components.

Effect of NodRm-IV(Ac,S) on root hair membrane potential and currents

A typical example of the E_m recording of a root hair from a plantlet treated with 4×10^{-8} M Nod factor is shown in Figure 1(A). Whatever the ion current signature, Nod factor induces a temporary depolarization. The membrane repolarized in the presence of Nod factor and even hyperpolarized slowly (relative to the E_m value recorded before Nod factor addition, Figure 1A,B). The same typical electrical behaviour, depolarization–hyperpolarization, could be observed using vanadate (500 μM), a classical H^+ pump inhibitor, or A23187 (5 μM), a calcium ionophore known to mimic the effect of Nod factor (Felle *et al.*, 1998). Tetraacetylchitotetraose (TACT, 4×10^{-7} M), a molecule

representing the Nod factor backbone which has no effect on the E_m (Kurkdjian, 1995), was used as a negative control (Figure 1B).

Role of IIAC

In order to study the role of the anion channel current in Nod factor signalling, we used root hairs showing predominantly IIAC. The inward current intensity elicited at –200 mV was measured at different time points during the E_m recording, i.e. (a) before Nod factor addition, (b) at optimal depolarization (after about 3 min), and (c) at hyperpolarization (Figure 2A). Figure 2(B) shows the kinetics of these anion currents. The positive values of activation potentials (i.e. near the estimated E_A–) (Figure 2C) and the instantaneous activation of the current (Figure 2B) are consistent with the anion nature of the current. As indicated (Figure 2A–C), the anion current increase was transient; the inward current intensity increased during depolarization (the first 3 min of Nod factor action) and then decreased during repolarization, with this decrease continuing during membrane hyperpolarization.

Using vanadate or A23187, the current variations recorded at the maximal depolarization and at the maximal hyperpolarization evolved in the same ways as those induced by Nod factor. TACT had no effect on the current (Figure 2D).

Role of IRKC

In order to study the role of K^+ channel current in Nod factor signalling, we used root hairs showing predominantly IRKC. The inward current intensity elicited at –200 mV was measured at different time points during the E_m recording (Figure 3A). Figure 3(B) shows the time-dependent kinetics of the inward K^+ currents activated at –200 mV for the three specific time points of the E_m recording, i.e. (a) before Nod factor addition, (b) at optimal depolarization, and (c) at hyperpolarization. The fact that the I–V curves (Figure 3C) show negative values of activation potentials for the inward functioning of the channels (near the estimated E_K) and also time-dependent activation, is consistent with the K^+ nature of this current. Note that these inward K^+ channels could represent an efflux pathway for K^+ at potentials positive to E_K. As indicated (Figure 3A–C), the increase of the K^+ inward current was transient, with the intensity increasing during the depolarization and then decreasing during the phase of repolarization–hyperpolarization.

Preliminary results showed that A23187 also induced a transient increase of IRKC during the depolarization which was followed by a decrease of this current during the hyperpolarization (not shown); unfortunately, because of the low frequency of recordings with predominant IRKC (6% of the root hairs tested), this could not be fully explored.

Effect of NodRm-IV(Ac,S) when both IRKC and IIAC are present

We checked the role of the anion and potassium channel currents in Nod factor signalling for root hairs showing both IIAC and IRKC. The total inward current intensity was measured at the same time points as for the E_m recording (Figure 4A). Figure 4(B) shows the kinetics of these currents with both a large instantaneous component and a time-dependent component. The positive values of activation potentials for the total current and IIAC (Figure 4C) indicate that the activation potential of the total current is imposed by the IIAC. The negative activation potential of the time-dependent current (Figure 4C) is consistent with its potassium nature. As indicated in Figure 4(C), the current increase upon Nod factor addition was transient; the inward current intensity increased during the depolarization and then decreased during the repolarization. This behaviour is the same for the IIAC and the IRKC, as previously described for root hairs displaying only one component predominantly (see Figures 2 and 3).

Role of the H^+ pump

The role of the H^+ pump was also investigated in the Nod-factor-induced electrical response. The Nod factor depolarization was compared to the one induced by two H^+-ATPase inhibitors and by one metabolic inhibitor. Erythrosin B, an H^+-ATPase inhibitor when used at relatively high concentration (50 μM) (Rasi-Caldogno *et al.*, 1989), induced a depolarization which was of the same order of magnitude as the one induced by vanadate at optimal concentration (500 or 1000 μM) (Figure 5A). The depolarizations induced by inhibition of the H^+ pump were reversible in the presence of the inhibitors (data not shown). By contrast, the metabolic inhibitor sodium azide (2 mM) induced a depolarization of much higher amplitude (Figure 5A) which was reversible when the inhibitor was washed out.

When root hairs were treated with 100 μM or 250 μM vanadate, the addition of 4×10^{-8} M Nod factor induced a larger depolarization (Figure 5A) which reached the amplitude recorded with optimal vanadate concentrations. In the presence of 500 μM vanadate inducing optimal depolarization, Nod factor did not produce any additional depolarization. All these results are consistent with the hypothesis of blocking of the H^+ pump during the early Nod factor response.

However, due to the potential inhibition by vanadate of the Ca^{2+} pumps (Giannini *et al.*, 1987), we tried to analyse

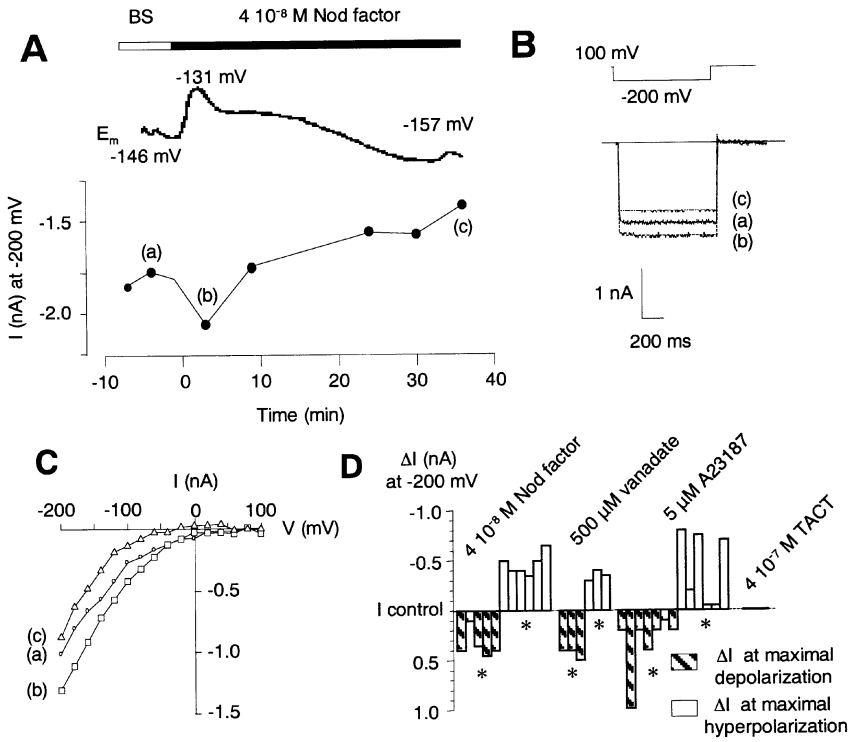

Figure 2. Nod-factor-induced changes in anion currents (IIAC) in a *Medicago* root hair.
Same experimental conditions as for Figure 1. The bar illustrates the time when Nod factor (4×10^{-8} M) was added to the bath solution.
(A) Recording of the membrane potential (E_m) and corresponding amplitude of current elicited at –200 mV.
(B) Voltage protocol. The instantaneously activated currents were measured before Nod factor addition (a), at optimal depolarization (b) and at hyperpolarization (c).
(C) Current–voltage relationships. The steady-state current amplitudes (after leak subtraction) were measured at membrane potentials ranging from –200 to +100 mV for the three specific time points of the E_m recording as indicated in (B).
(D) Variations of inward currents (ΔI) at maximal depolarization and at maximal hyperpolarization after treatment with Nod factor (4×10^{-8} M), vanadate (500 µM) or A23187 (5 µM). *Significantly different from TACT (4×10^{-7} M)-treated root hair currents ($P < 0.05$).

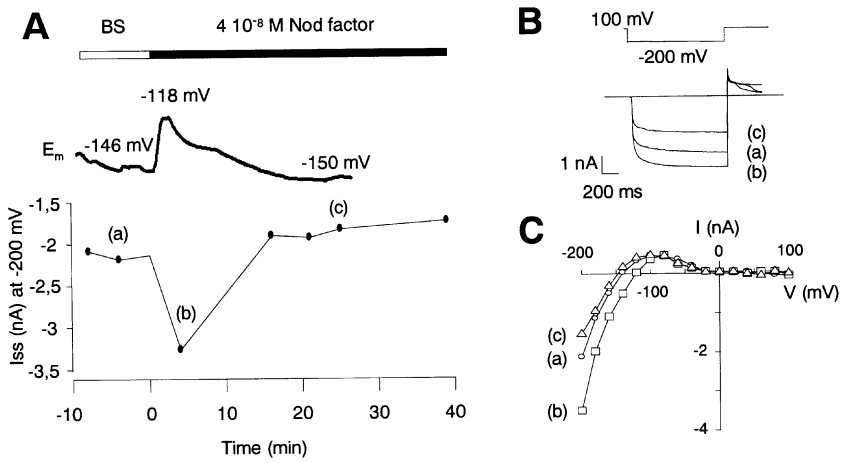

Figure 3. Nod-factor-induced changes in inward K^+ currents (IRKC) in a *Medicago* root hair.
Same experimental conditions as for Figure 1. The bar illustrates the time when Nod factor (4×10^{-8} M) was added to the bath solution.
(A) Recording of the membrane potential (E_m) and corresponding time-dependent current kinetics. The steady-state current amplitudes were measured for the same voltage conditions as for Figure 2. The data are representative for five cells showing the same trends in current patterns, although the total magnitude of change varied widely.
(B) Same voltage protocol as for Figure 2. The currents were measured at the specific time points defined in Figure 2(B).
(C) Current–voltage relationships.

directly the H^+ pump current in response to Nod factor. Voltage-independent variations of outward currents were recorded at potentials positive to the activation potentials of IRKC and IIAC (positive to +50 mV). These variations were assumed to correspond to variations of the H^+ pump current consistent with its inhibition by vanadate (500 µM) and stimulation by the fungal toxin fusicoccin (10 µM) (Marré, 1979) (Figure 5B), and to the classical description of H^+ pump functioning (Blatt, 1987; Spanswick, 1981). As indicated in Figure 5(C), Nod factor induced a decrease of the H^+ pump current during the depolarization, whereas the H^+ pump was stimulated during the hyperpolarization. Although the variations of the H^+ pump current were low, they were always of the same nature for Nod factor or A23187 (i.e. inhibition and then stimulation). In contrast, vanadate induced a decrease of this current during the depolarization but also during the repolarization phase (Figure 5B); fusicoccin only increased this current (Figure 5B). As described for the anion current, TACT did not modify the H^+ pump current (Figure 5C).

Role of calcium

The internal Ca^{2+} is implicated in the early phase of Nod factor signalling (Cardenas *et al.*, 1999; Felle *et al.*, 1998, 1999; Gehring *et al.*, 1997; Pingret *et al.*, 1998) and H^+ pump

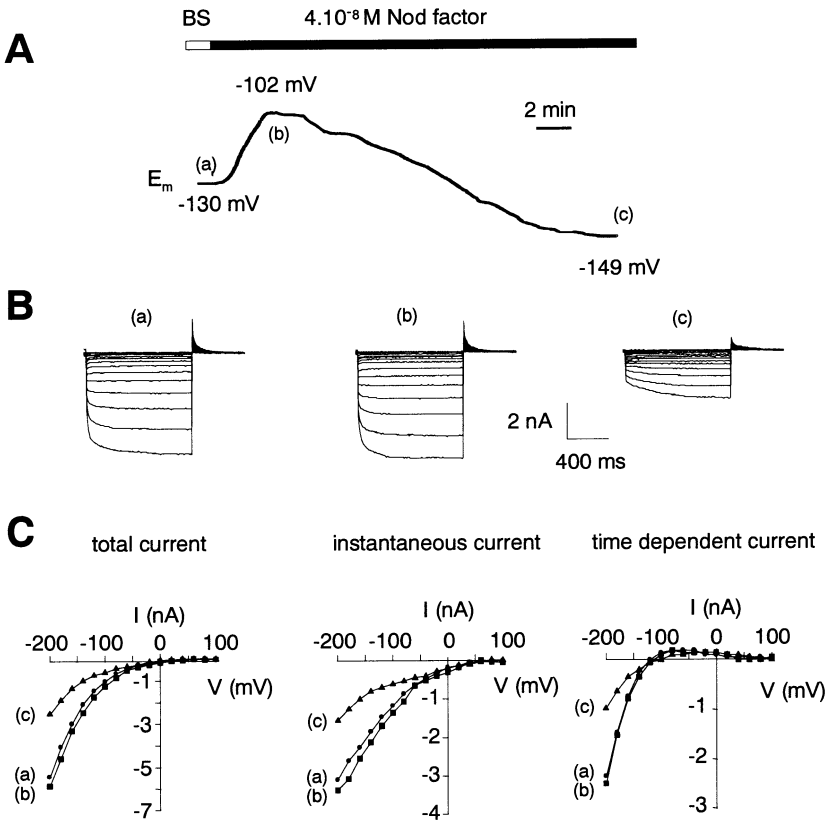

Figure 4. Nod-factor induced changes in total inward currents (IRKC + IIAC) in a *Medicago* root hair.
Same experimental conditions as for Figure 1. The bar illustrates the time when Nod factor (4×10^{-8} M) was added to the bath solution.
(A) Recording of the membrane potential (E_m).
(B) Voltage protocol. The currents were measured at the specific time points defined in Figure 2(B).
(C) Current–voltage relationships for the total current, for the instantaneous current and for the steady-state time-dependent current. The data are representative for three cells showing the same trends in current patterns, although the total magnitude of change varied widely.

blocking (Kinoshita *et al.*, 1995; Lino *et al.*, 1998; Marré and Ballarin-Denti, 1985). Because A23187 mimicks the effect of Nod factor on E_m (Felle *et al.*, 1998) (Figure 6A), on anion currents (Figure 2D) and on the H^+ pump current (Figure 5B), we further investigated the role of Ca^{2+} using La^{3+}, a Ca^{2+} channel blocker. When root hairs were treated with La^{3+} (125 μM), the addition of Nod factor did not induce the typical electrical response (Figure 6B). Also, experiments where Mg^{2+} was substituted for Ca^{2+} in the bath solution indicated that Nod factor had no significant effect on membrane polarization (Figure 6C). These results suggest, as do those of other authors, that an influx of calcium across the plasma membrane could be necessary for the Nod-factor-induced depolarization.

Discussion

The aim of this work was to identify the nature of the ion currents involved in the Nod factor signalling process evoking the well-known depolarization (Ehrhardt *et al.*, 1992; Felle *et al.*, 1995; Kurkdjian, 1995). We showed that the early membrane depolarization involves a decrease of the H^+ pump current (efflux of positive charges), an increase of inward K^+ channel currents (IRKC) (influx of positive charges) and an increase of inward anion channel currents (IIAC) (efflux of negative charges) in root hairs of *M. sativa.* These three currents were then conversely regulated to allow membrane repolarization.

Nod factor induces a transient increase of the anion inward current (anion efflux) which is then decreased, following the E_m variation. These results are in agreement with those of Felle *et al.* (1998) showing the transient increase of anion efflux in response to Nod factor with kinetics similar to those reported here. For root hairs showing predominantly the IRKC, the Nod factor induces an early increase of the inward K^+ current which can participate in the depolarization. This current is then decreased during the repolarization. A variation of K^+ influx was not revealed by Felle *et al.* (1998) using K^+-selective microelectrodes located in the buffer solution close to sensitive root hairs. However, these authors showed (during the lapse of time between Nod factor addition and the induced K^+ efflux) a slight decrease of the apoplasmic K^+ concentration (see Figure 5 in Felle *et al.*, 1998), i.e. a K^+ influx (Felle, personal communication) corresponding to the early increase of IRKC we recorded. As our experiments were performed at physiological external pH (pH 6) (Grignon and Sentenac, 1991), this could facilitate observation of the increase in IRKC compared to external neutral pH conditions as used by Felle *et al.* (1998) which are known to decrease the inward K^+ current (Blatt, 1992; Brüggemann *et al.*, 1999).

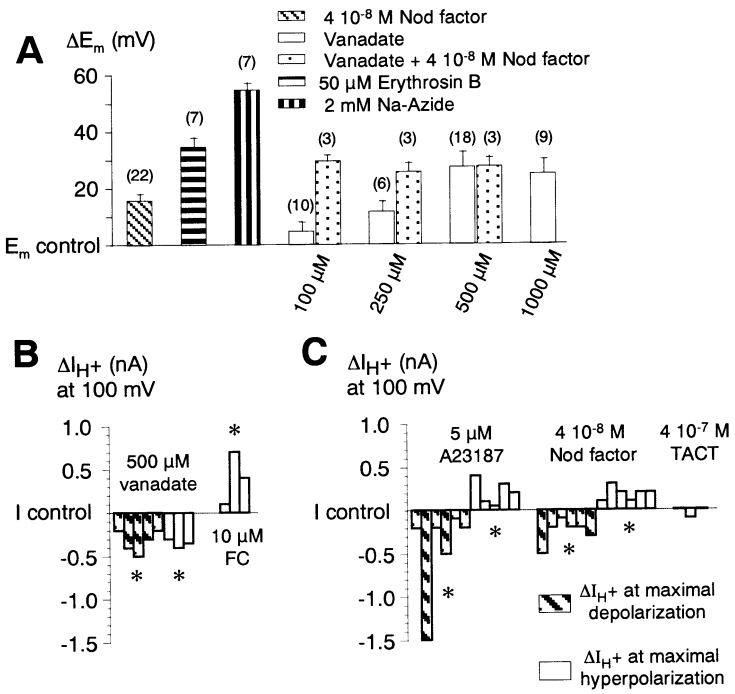

Figure 5. Nod-factor-induced changes in the plasma membrane H^+-ATPase pump current in a *Medicago* root hair.
Same experimental conditions as for Figure 1.
(A) E_m was recorded, and at equilibrium Nod factor (4×10^{-8} M), erythrosin B (50 µM) or sodium azide (2 mM) were perfused. Alternatively, vanadate at concentrations ranging from 100 to 1000 µM was perfused, and, at maximal depolarization, Nod factor was added. ΔE_m (mV) correspond to the maximal amplitudes of depolarization induced by the effectors.
(B) Pharmacological H^+ pump current characterization without Nod factor. ΔI (calculated at +100 mV) corresponds to the current amplitudes of maximal depolarization and/or hyperpolarization after treatment with vanadate (500 µM) and fusicoccin (FC) (10 µM).
(C) Effect of Nod factor, A23187 (5 µM) and TACT (4×10^{-7} M) on H^+ pump current. ΔI (calculated at +100 mV) corresponds to the current amplitudes of maximal depolarization and hyperpolarization. *Significantly different from TACT (4×10^{-7} M)-treated root hair currents ($P < 0.05$).

Furthermore, the measurements of Felle *et al.* (1998) were performed in the volume located between root hairs; for this reason, they concern several root hairs which did not necessarily display the same pattern of IRKC, according to our previous observations (Bouteau *et al.*, 1999).

However, during Nod-factor-induced depolarization, the IRKC could allow a K^+ efflux for potential values positive to E_K (Bouteau *et al.*, 1999), as recently described for KAT1 currents (Brüggemann *et al.*, 1999). This K^+ efflux through IRKC channels is here in accordance with the delayed K^+ efflux recorded with K^+-selective microelectrodes (Felle *et al.*, 1998), as they showed that external K^+ concentration starts to increase at the exact time that the depolarization passes E_K, i.e. when the K^+ motive force changes from being inwardly to outwardly directed.

In plant cells, potassium effluxes are supposed to mainly occur through K^+ outward-rectifying channels (Jeannette *et al.*, 1999; Maathuis *et al.*, 1997) or non-selective outward cation channels (Wegner and De Boer, 1997). However, under our conditions, the ORKC was rarely observed and it should not contribute to membrane repolarization since its activation potential is more positive (–95 mV) (Bouteau *et al.*, 1999) than the mean E_m reached during Nod-factor-induced depolarization (about –110 mV).

The inhibitory effect of vanadate on the H^+-ATPase is well established for plant cells *in vivo* and for plasma membrane vesicles (Sze, 1984 and refs therein). However, vanadate seemed also to be a potent inhibitor of the Ca^{2+} pumps (Giannini *et al.*, 1987). Thus, in order to reinforce the pharmacological study, we directly analysed the H^+ pump current in response to Nod factor. In the short term, vanadate rapidly inhibits *Medicago* root hair proton pumping (Figure 5A,B). Furthermore, we showed that, in the presence of vanadate, Nod factor is only efficient in depolarizing the membrane if the H^+ pump is not strongly inhibited (see Figure 5A), emphasizing the role played by the pump in the Nod factor signalling. Analysis of the H^+ pump current variations in response to Nod factor (Figure 5B) shows that the inhibition is transient, i.e. the current decreases during the depolarization and is stimulated during the hyperpolarization. This last event agrees with the alkalinization of the apoplasm recorded with H^+-selective microelectrodes (Allen *et al.*, 1994; Felle *et al.*, 1998). We have shown that A23187 induces IIAC variations in the same direction as Nod factor. The calcium ionophore also mimicked the Nod factor effect on the H^+ pump current during all E_m variations (Figure 5B), whereas vanadate inhibited the H^+ pump current even when the root hair membrane ultimately hyperpolarized.

The effect of A23187 on the polarization of root hairs is certainly linked to an intracellular calcium increase as in the case of Nod factor (Cardenas *et al.*, 1999; Felle *et al.*, 1998; Felle *et al.*, 1999; Gehring *et al.*, 1997; Pingret *et al.*, 1998). Furthermore, inhibition of the Nod-factor-induced depolarization using La^{3+}, a Ca^{2+} channel blocker (Figure 6B), or Mg^{2+} as a substitute for Ca^{2+} (Figure 6C), strongly suggests that the calcium increase in the cytoplasm comes from the extracellular medium even though its concomitant release from internal stores cannot be excluded as observed for hypo-osmotic shock (Cessna *et al.*, 1998). The regulation of the calcium level by the Ca^{2+} pump could explain the repolarization observed after the

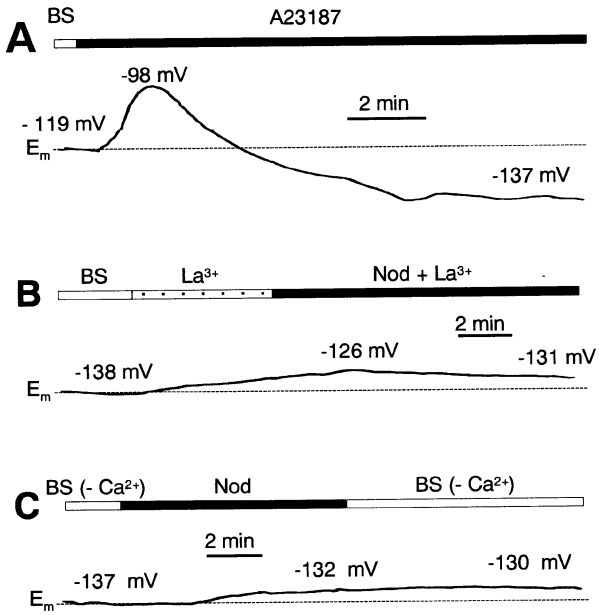

Figure 6. Role of calcium in Nod-factor-induced changes in the electrical membrane potential.
(A–C) Recordings of E_m. Whole plantlets (29 h old) were perfused with standard buffer solution (BS containing 1 mM $CaSO_4$) (pH 6.0). The bars illustrate the time that the effectors (A23187, 5 μM; $LaCl_3$, 125 μM; Nod factor 4×10^{-8} M) were added to the bath solution (BS).
(A) Effect of the calcium ionophore A23187 on E_m. Results are representative of seven separate experiments.
(B) Effect of a calcium channel inhibitor. $LaCl_3$ was perfused for a few minutes before the addition of Nod factor (4×10^{-8} M). Results are representative of four separate experiments.
(C) Effect of calcium substitution by magnesium. The plantlet was perfused with the standard buffer solution containing $MgSO_4$ (1 mM) and no calcium. Nod factor (4×10^{-8} M) was perfused and then eliminated. Results are representative of two separate experiments.

Nod factor and the A23187-induced depolarization (Felle *et al.*, 1992). Other studies concerning various membrane signalling events implicate this kind of regulation (Cramer and Jones, 1996). The hypothesis of a vanadate-induced increase of internal Ca^{2+} can be raised owing to the potential inhibition by vanadate of the Ca^{2+} pumps (P-type Ca^{2+} and H^+-ATPases) as observed in plasma membrane vesicles from red beet storage tissue (Giannini *et al.*, 1987). This could explain the root hair repolarization in the presence of vanadate by a Ca^{2+}-dependent IIAC decrease.

In conclusion, our results suggest that the inward current increase induced by Nod factor may be due to an anion efflux and/or a K^+ influx, responsible for the early depolarization, suggesting a weak specificity for this step of signal transduction. Subsequently, the delayed K^+ efflux could occur through the inward-rectifying K^+ channels which function outwards for E_m positive to E_K. These results are in agreement with the hypothetical models proposed for the Nod factor signalling pathway by Felle *et al.* (1998) and with the classical response to elicitors, namely extracellular alkalinization, influx of calcium and efflux of chloride and potassium ions (Hebe *et al.*, 1999; Nürnberger *et al.*, 1997). However, it is established that cells must integrate signals from a range of often conflicting stimuli, many of them using Ca^{2+} as a second messenger. This fact raises questions about the mechanisms by which root hairs discriminate between different Ca^{2+} stimuli. It remains to be shown which elements of the signal transduction cascade are modulated in a specific way to allow the plant cell to discriminate between an elicitor of plant defence and a symbiotic signal.

Experimental procedures

Plant material

Alfalfa seeds (*Medicago sativa* cv Sitel) were grown as previously described (Kurkdjian, 1995). Whole plantlets (about 30 h old) were mounted on slides and constantly perfused with the standard buffer solution (BS) consisting of 5 mM MES buffered to pH 6.0 (pH 5.5 for vanadate experiments) with 5 mM Tris, containing 0.1 mM KCl and 1 mM $CaSO_4$. The experiments were carried out at room temperature. Young growing root hairs, 5–20 μm long (zone 1 according to Heidstra *et al.*, 1994; de Ruijter *et al.*, 1998) were chosen because they have been reported to be the more sensitive to Nod factor in terms of root hair deformation and the electrical membrane response (Geurtz and Franssen, 1996; Kurkdjian, 1995).

Effectors and chemicals

A stock solution of Nod factor, NodRm-IV(Ac, S), was prepared as described earlier (Kurkdjian, 1995). Synthetic *N,N′,N″,N‴*-tetra-acetylchitotetraose (TACT) was dissolved in double-distilled H_2O as a stock solution (1 mM) and kept frozen at –20°C. Ammonium metavanadate (NH_4VO_3) was prepared as a fresh stock solution (10 mM) in Tris-MES buffer (pH 5.5). We have checked that NH_4^+ (1 mM) does not significantly modify E_m. Erythrosin B and $LaCl_3$ were prepared as 10 mM stock solutions in bi-distilled H_2O. NaN_3 was prepared as a 100 mM stock solution in bi-distilled H_2O. A23187 was dissolved as 10 mM stock solution in ethanol. We have checked that the ethanol concentration used (1/10 000) had no effect on the currents.

Electrophysiology

Voltage-clamp measurements were carried out using a discontinuous single voltage-clamp microelectrode technique (Finkel and Redman, 1985) to record the currents from intact root hairs (Bouteau *et al.*, 1999). Specific software (pCLAMP5.5, Axon Instruments, Foster City, CA, USA) drives the electrometer. Microelectrodes were made from borosilicate capillary glass (Clark GC 150F, Clark Electromedical, Pangbourne, Reading, UK) and filled with 600 mM KCl. Electrical resistances were 50–100 MΩ in the buffer solution. The electrode was connected to an electrometer (Axoclamp 2A, Axon Instruments). Voltage and current were displayed on a dual input oscilloscope (Gould 1425, Gould Instruments Ltd, Hainault, UK), digitalized with a PC computer that was fitted with an acquisition board (Labmaster TL 1, Scientific Solutions Inc., Solon, OH, USA). The

opening or closure of the channels was achieved as indicated in the figures, with protocols of 20 mV steps, during 500 or 1000 ms, with a resting phase of 500 or 1000 ms at the holding potential. We systematically checked to ensure that root hairs were correctly clamped by comparing the protocol voltage values with those actually imposed. Only a small percentage of root hairs failed to display a linear relationship between theoretical and measured potentials. These root hairs were then abandoned.

Presentation of data

Kinetics are given as single measurements, representative of a number of equivalent tests carried out under the same conditions, as indicated in the figure legends. For current kinetics and I–V curves, the leak resistance was subtracted. For IRKC analysis, the instantaneous current was subtracted from the steady-state current to ensure that only the time-dependent current was considered (cf. Bouteau *et al.*, 1999). Membrane potential data are given as means ± SD. Due to small sample size and the variability of current recordings, their values were compared using TACT as a negative control with a unilateral-non-parametric test, the Willcoxon rank-sum test. A value of $P<0.05$ was considered as significant.

Acknowledgements

We thank Professor J. Dénarié for the gift of the *O*-acetylated Nod factor. We greatly acknowledge Dr H. Barbier-Brygoo and O. Dellis for critical reading of the manuscript and for fruitful discussions. We wish also to thank Dr S. Brown for correcting the English. This work was supported by grants from DRED (Direction de la Recherche et des Etudes Doctorales, Ministère de l'Education Nationale et de la Culture, EA291) and from the Centre National de la Recherche Scientifique (UPR 0040) to A.K.

References

Allen, N.S., Bennet, M.N., Cox, D., Shipley, A., Ehrhardt, D. and Long, S.R. (1994) Effects of Nod-factors on alfalfa root hair Ca^{2+} and H^+ currents and cytoskeleton behaviour. In *Advances in Molecular Genetics of Plant–Microbe Interactions* (Daniels, M.G., Downie J.A. and Osborne, A.E., eds). Dordrecht: Kluwer, pp. 107–114.

Bauer, P., Poirier, S., Ratet, P. and Kondorosi, A. (1997) MsEnod 12A expression is linked to meristematic activity during development of indeterminate and determinate nodules and roots. *Mol. Plant–Microbe Interact.* **10**, 39–49.

Blatt, M.R. (1987) Electrical characteristics of stomatal guard cells: the contribution of ATP-dependent, 'electrogenic' transport revealed by current–voltage and difference–current–voltage analysis. *J. Membr. Biol.* **98**, 257–274.

Blatt, M.R. (1992) K^+ channels of stomatal guard cells. *J. Gen. Physiol.* **99**, 615–644.

Bouteau, F., Pennarun, A.M., Kurkdjian, A., Convert, M., Cornel, D., Monestiez, M., Rona, J.P. and Bousquet, U. (1999) Ion channels of young root hairs from *Medicago sativa*. *Plant Physiol. Biochem.* **37**, 889–898.

Brüggemann, L., Dietrich, P., Becker, D., Dreyer, I., Palme, K. and Hedrich, R. (1999) Channel-mediated high-affinity K^+ uptake into guard cells from *Arabidopsis*. *Proc. Natl Acad. Sci. USA*, **96**, 3298–3302.

Cardenas, L., Vidali, L., Dominguez, J., Pérez, H., Sanchez, F., Hepler, P.K. and Quinto, C. (1998) Rearrangement of actin microfilaments in plant root hairs responding to *Rhizobium etli* nodulation signals. *Plant Physiol.* **116**, 871–877.

Cardenas, L., Feijo, J.A., Kunkel, J.G., Sanchez, F., Holdaway-Clarke, T., Hepler, P.K. and Quinto, C. (1999) *Rhizobium* Nod factors induce increases in intracellular free calcium influxes in bean root hairs. *Plant J.* **19**, 347–352.

Cessna, S.G., Chandra, S. and Low, P.S. (1998) Hypo-osmotic shock of tobacco cells stimulates Ca^{2+} fluxes deriving first from external and then internal Ca^{2+} stores. *J. Biol. Chem.* **273**, 27286–27291.

Cramer, G.R. and Jones, R.L. (1996) Osmotic stress and abscisic acid reduce cytosolic calcium activities in roots of *Arabidopsis thaliana*. *Plant Cell Environ.* **19**, 1291–1298.

Ehrhardt, D.W., Atkinson, E.M. and Long, S.R. (1992) Depolarization of alfalfa root hair membrane potential by *Rhizobium meliloti* Nod-factors. *Science*, **256**, 998–1000.

Ehrhardt, D.W., Wais, R. and Long, S.R. (1996). Calcium spiking in plant root hairs responding to *Rhizobium* nodulation signals. *Cell*, **85**, 673–681.

Felle, H.H., Tretyn, A. and Wagner, G. (1992) The role of the plasma-membrane Ca^{2+}-ATPase in Ca^{2+} homeostasis in *Sinapis alba* root hairs. *Planta*, **188**, 306–313.

Felle, H.H., Kondorosi, E., Kondorosi, A. and Schultze, M. (1995) Nod signal-induced plasma membrane potential changes in alfalfa root hairs are differentially sensitive to structural modifications of the lipo chitooligosaccharide. *Plant J.* **7**, 101–109.

Felle, H.H., Kondorosi, E., Kondorosi, A. and Schultze, M. (1998) The role of ion fluxes in Nod-factor signalling in *Medicago sativa*. *Plant J.* **13**, 455–463.

Felle, H.H., Kondorosi, E., Kondorosi, A. and Schultze, M. (1999) Elevation of the cytosolic free $[Ca^{2+}]$ is indispensable for the transduction of the Nod factor signal in alfalfa. *Plant Physiol.* **121**, 273–279.

Finkel, A.S. and Redman, S.J. (1985) Optimal voltage clamping with single electrode. In *Voltage and Patch Clamping with Microelectrodes* (Smith, T.G. Jr, Locar, H. Jr, Redman, S.J. and Gage, P.W., eds), American Physiological Society, pp. 95–120.

Gehring, C.A., Irving, H.R., Kabbara, A.A., Parish, R.W., Boukli, N.M. and Broughton, W.J. (1997) Rapid, plateau-like increases in intracellular free calcium are associated with Nod-factor-induced root hair deformation. *Mol. Plant–Microbe Interact.* **10**, 791–802.

Geurts, R. and Franssen, H. (1996) Signal transduction in *Rhizobium*-induced nodule formation. *Plant Physiol.* **112**, 447–453.

Giannini, J.L., Ruiz-Cristin, J. and Briskin, D.P. (1987) Calcium transport in sealed vesicles from red beet (*Beta vulgaris* L.) storage tissue. II. Characterization of $^{45}Ca^{2+}$ uptake into plasma membrane vesicles. *Plant Physiol.* **85**, 1137–1142.

Grignon, C. and Sentenac, H. (1991) pH and ionic conditions in the apoplast. *Annu. Rev. Plant Physiol. Plant Mol Biol.* **42**, 103–128.

Hebe, G., Hager, A. and Salzer, P. (1999) Initial signalling processes induced by elicitors of ectomycorrhiza-forming fungi in spruce cell can also triggered G-protein-activating mastosporan and protein phosphatase-inhibiting cantharidin. *Planta*, **207**, 418–425.

Heidstra, R., Geurts, R., Franssen, H., Spaink, H.P., van Kammen, A. and Bisseling, T. (1994) Root hair deformation activity of nodulation factors and their fate on *Vicia sativa*. *Plant Physiol.* **105**, 787–797.

Horvath, B., Heidstra, R., Lados, M., Moerman, M., Spaink, H.P., Promé, J.C., Van Kammen, A. and Bisseling, T. (1993)

Lipooligosaccharides of *Rhizobium* induce infection-related early nodulin gene expression in pea root hairs. *Plant J.* **4**, 723–733.

Jeannette, E., Rona, J.P., Bardat, F., Cornel, D., Sotta, B. and Miginiac, E. (1999) Induction of RAB18 gene expression and activation of K^+ outward rectifying channels depend on an extracellular perception of ABA in *Arabidopsis thaliana* suspension cells. *Plant J.* **18**, 13–22.

Journet, E.P., Pichon, M., Dedieu, A., De Billy, F., Truchet, G. and Barker, D.G. (1994) *Rhizobium meliloti* Nod-factors elicit cell-specific transcription of the *ENOD*12 gene in transgenic alfalfa. *Plant J.* **6**, 241–249.

Kinoshita, T., Nishimura, M. and Shimazaki, K. (1995) Cytosolic concentration of Ca^{2+} regulates the plasma membrane H^+-ATPase in guard cells of fava bean. *Plant Cell*, **7**, 1333–1342.

Kurkdjian, A. (1995) Role of the differentiation of root epidermal cells in Nod-factor (from *Rhizobium meliloti*) induced root hair depolarization of *Medicago sativa*. *Plant Physiol.* **107**, 783–790.

Lerouge, P., Roche, P., Faucher, C., Maillet, F., Truchet, G., Promé, J.C. and Dénarié, J. (1990) Symbiotic-host specificity of *Rhizobium meliloti* is determined by a sulphated and acylated glucosamine oligosaccharide signal. *Nature*, **344**, 781–784.

Lino, B., Baizabal-Aguirre, V.M. and Gonzales de la Vera, L.E. (1998) The plasma-membrane H^+-ATPase from sugar beet root is inhibited by a calcium-dependent phosphorylation. *Planta*, **204**, 352–359.

Long, S.R. (1996) *Rhizobium* symbiosis: Nod-factors in perspective. *Plant Cell*, **8**, 1885–1898.

Maathuis, F.J.M., Ichida, A.M., Sanders, D. and Schroeder, J.I. (1997) Roles of higher plant K^+ channels. *Plant Physiol.* **114**, 1141–1149.

Marré, E. (1979) Fusicoccin: a tool in plant physiology. *Annu. Rev. Plant Physiol.* **30**, 273–288.

Marré, E. and Ballarin-Denti, A. (1985) The proton pumps of the plasmalemma and the tonoplast of higher plants. *J. Bioenerg. Biomembr.* **17**, 1–21.

Mylona, P., Pawlowski, K. and Bisseling, T. (1995) Symbiotic nitrogen fixation. *Plant Cell*, **7**, 869–885.

Niebel, A., Bono, J.J., Ranjeva, R. and Cullimore, J.V. (1997) Identification of a high affinity binding site for lipo-oligosaccharidic NodRm factors in the microsomal fraction of *Medicago* cell suspension cultures. *Mol. Plant–Microbe Interact.* **10**, 132–134.

Nürnberger, T., Wirtz, W., Nennstiel, D., Hahlbrock, K., Jabs, T., Zimmermann, S. and Scheel, D. (1997). Signal perception and intracellular signal transduction in plant pathogen defense. *J. Receptor Signal Transduction Res.* **17**, 127–136.

Pingret, J.L., Journet, E.P. and Barker, D.G. (1998) *Rhizobium* Nod-factor signaling: evidence for a G protein-mediated transduction mechanism. *Plant Cell*, **10**, 659–671.

Rasi-Caldogno, F., Pugliarello, M.C., Olivari, C. and De Michelis, M.I. (1989) Identification and characterization of the Ca^{2+}-ATPase which drives active transport of Ca^{2+} at the plasma membrane of radish seedlings. *Plant Cell*, **5**, 523–530.

Relic, B., Perret, X., Estrada-Garcia, M.T., Kopcinska, J., Golinowski, W., Krishnan, H.B., Pueppke, S.G. and Broughton, W.J. (1994) Nod factors of *Rhizobium* are key to the legume donor. *Mol. Microbiol.* **13**, 171–178.

de Ruijter, N.C.A., Rook, M.B., Bisseling, T. and Emons, A.M.C. (1998) Lipochito-oligosaccharides re-initiate root hair tip growth in *Vicia sativa* with high calcium and spectrin-like antigen at the tip. *Plant J.* **13**, 341–350.

de Ruijter, N.C.A., Bisseling, T. and Emons, A.M.C. (1999) Rhizobium Nod factors induce an increase in sub-apical fine bundles of actin filaments in *Vicia sativa* root hairs within minutes. *Mol. Plant–Microbe Interact.* **12**, 829–832.

Schultze, M., Quiclet-Sire, B., Kondorosi, E., Virelizier, H., Glushka, J., Endre, G., Gero, S.D. and Kondorosi, A. (1992) *Rhizobium meliloti* produces a family of sulfated lipooligosaccharides exhibiting different degrees of plant host specificity. *Proc. Natl Acad. Sci. USA*, **89**, 192–196.

Spaink, H.P., Sheeley, D.M., Van Brussel, A.A.N., Glushka, J., York, W.S., Tak, T., Geiger, O., Kennedy, E.P., Reinhold, V.N. and Lugtenberg, B.J.J. (1991) A novel highly unsaturated fatty acid moiety of lipo-oligosaccharide signals determines host specificity of *Rhizobium*. *Nature*, **354**, 125–130.

Spanswick, R.M. (1981) Electrogenic ion pumps. *Annu. Rev. Plant Physiol.* **32**, 267–289.

Sze, H. (1984) H^+-translocating ATPases of the plasma membrane and tonoplast of plant cells. *Physiol. Plant.* **61**, 683–691.

Truchet, G., Roche, P., Lerouge, P., Vasse, J., Camut, S., De Billy, F., Promé, J.C. and Dénarié, J. (1991) Sulphated lipo-oligosaccharide signals of *Rhizobium meliloti* elicit root nodule organogenesis in alfalfa. *Nature*, **351**, 670–673.

Ward, J.M. and Schroeder, J.I. (1997) Roles of ion channels in initiation of signal transduction in higher plants. In *Signal Transduction in Plants* (Aducci, P., ed.). Basel: Springer Verlag, pp. 1–22.

Wegner, L.H. and De Boer, A.H. (1997) Properties of two outward-rectifying channels in root xylem parenchyma cells suggest a role in K^+ homeostasis and long distance signaling. *Plant Physiol.* **115**, 1707–1719.